Effect of nitrogen doping on the electromagnetic properties of carbon nanotube-based composites

M. A. Kanygin, O. V. Sedelnikova, I. P. Asanov, L. G. Bulusheva, A. V. Okotrub et al.

Citation: J. Appl. Phys. **113**, 144315 (2013); doi: 10.1063/1.4800897
View online: http://dx.doi.org/10.1063/1.4800897
View Table of Contents: http://jap.aip.org/resource/1/JAPIAU/v113/i14
Published by the American Institute of Physics.

JOURNAL OF APPLIED PHYSICS **113**, 144315 (2013)

Effect of nitrogen doping on the electromagnetic properties of carbon nanotube-based composites

M. A. Kanygin,[1] O. V. Sedelnikova,[1] I. P. Asanov,[1] L. G. Bulusheva,[1] A. V. Okotrub,[1] P. P. Kuzhir,[2,a)] A. O. Plyushch,[2] S. A. Maksimenko,[2] K. N. Lapko,[3] A. A. Sokol,[3] O. A. Ivashkevich,[3] and Ph. Lambin[4]
[1]*Nikolaev Institute of Inorganic Chemistry, SB RAS, 3 Acad. Lavrentiev av., 630090 Novosibirsk, Russia*
[2]*Research Institute for Nuclear Problems of Belarusian State University, 11 Bobruiskaya str., 220030 Minsk, Belarus*
[3]*Belarusian State University, 14 Leningradskaya str., 220030 Minsk, Belarus*
[4]*Physics Department, FUNDP—University of Namur, 61 rue de Bruxelles, 5000 Namur, Belgium*

(Received 4 February 2013; accepted 25 March 2013; published online 12 April 2013)

Nitrogen-doped and pure carbon nanotube (CNT) based composites were fabricated for investigating their dielectric properties in static regime as well as electromagnetic response properties in microwave frequency range (K_a-band). Two classes of host matrix—polystyrene and phosphate unfired ceramics—have been used for composites fabrication. The study reveals miscellaneous effect of nitrogen doping on the dielectric permittivity, *dc* conductivity and electromagnetic interference shielding efficiency of CNT-based composites, produced with both polymer and ceramic matrices. The high-frequency polarizability, estimated for different-length CNTs, and static polarizability, calculated for nitrogen-containing CNT models using a quantum-chemical approach, show that this effect results from a decrease of the nanotube defect-free-length and deterioration of the polarizability with incorporation of nitrogen in pyridinic form. © *2013 AIP Publishing LLC* [http://dx.doi.org/10.1063/1.4800897]

I. INTRODUCTION

As the microwave spectrum becomes more crowded and "EM pollution" problem becomes more stressful, one needs effective multi-functional materials with high electrical conductivity and electromagnetic (EM) interference (EMI) shielding effectiveness (SE) for EM coatings, working in GHz frequency range. The conventional metallic shields, which are typically utilized to ensure the EM compatibility (EMC), have obvious disadvantages, such as large weight and thickness, and low corrosion resistance.

Recently, much attention has been focused on polymeric and ceramic composites filled with carbon nanotubes (CNTs). Being light, resistive to corrosion, showing multiple processing advantages, CNTs are widely investigated to overcome the aforementioned drawbacks and to supplement or even replace metals and metal foams for EMC applications (see reviews of Refs. 1 and 2 and references therein). The achievable range of the CNT-based composites EM properties can be very large[3] since either different nanotube types (single-walled (SWCNT), multi-walled (MWCNT), or their bundles) can be incorporated into the matrices, whereas different polymer/ceramics formulations and processing conditions may lead to different structures, which in turn do influence the physical properties of the resulting composites (see Ref. 4).

The most important parameters responsible for conductivity of CNT-based composites and their EM response properties are (i) the mass/volume fraction of CNT fillers relative to percolation threshold, (ii) the CNT filler dispersion state, and (iii) the polarizability of the individual tube (or bundle of tubes). The latter, according to Zhou *et al.*,[5] Khalfoun *et al.*,[6] and Ma *et al.*,[7] is influenced by the CNT purification degree, structural defects, doping, functionalization, etc. But generally, the polarizability was found by Li *et al.*[8] to be determined by the CNT length and aspect ratio, the volume occupied by electrons and the number of CNT atoms (see Ref. 9 and references therein). In the case of multi-shells structures, like MWCNTs, also the frequency range is very important. As it was shown by Zdrojek *et al.*,[10] Shuba *et al.*,[11] and Kuzhir *et al.*[12] that for some frequencies, not all the walls of MWCNTs indeed take part in the EM interaction, due to high internal EM screening.

Exohedral functionalization and structural modification may improve the CNT conductivity leading to the decrease of percolation threshold and the enhancement of EMI SE. In this respect, Czerw *et al.*,[13] Ewels and Glerup,[14] Villalpando-Paez *et al.*,[15] Ismagilov *et al.*,[16] Nemilentsau *et al.*,[17] Xu *et al.*,[18] and Latil *et al.*[19] mentioned CNT doping with nitrogen as being one of the most interesting.

The present communication is devoted to the effects nitrogen doping has on the electromagnetic properties of CNT-based composites in low-frequency and microwave (26–37.5 GHz) regions. The modeling of frequency-dependent polarizability *vs* nanotube geometrical parameters and quantum-chemical calculations of nitrogen-doped CNT (N-CNT) static polarizability are addressed in the paper in support to the observed experimental data.

II. EXPERIMENTAL DETAILS

A. CNT synthesis

Arrays of vertically aligned nanotubes were grown on silicon substrates by an aerosol-assisted catalytic chemical

a)Author to whom correspondence should be addressed. Electronic mail: polina.kuzhir@gmail.com, kuzhir@bsu.by

vapor deposition (CCVD) method described by Okotrub *et al.*[20] Pure and nitrogen-doped CNT samples were synthesized as the result of decomposition of 2 wt. % ferrocene solution in, respectively, toluene and acetonitrile at 800 and 850 °C.

Scanning electron microscopy (SEM) with a LEO-1455 VP microscope and transmission electron microscopy (TEM) with a JEOL-2010 microscope were used for structural characterization of samples. Concentration and chemical forms of nitrogen in N-MWCNTs were determined by X-ray photoelectron spectroscopy (XPS) using a Specslab PHOIBOS 150 spectrometer with monochromatic Al K_α radiation ($h\nu = 1486.6$ eV).

TEM micrographs show that the undoped CNTs have multi-walled structure with average outer diameter of ~20 nm (Fig. 1(a)). N-MWCNTs have a bamboo-like structure typical of nitrogen-doped nanotubes (see Refs. 21 and 22) and average outer diameter of ~50 nm (Fig. 1(b)). The concentration of nitrogen in N-MWCNTs is about 4 at. % as it was estimated from the ratio of areas of the N 1s and C 1s lines taking into account the photoionization cross sections. The N 1s XPS spectrum has three peaks located around 398.5 eV (I), 400.9 eV (II), and 405.0 eV (III). As it was shown by Kudashov *et al.*,[23] the peaks I and II can be attributed to the pyridinic and graphitic nitrogen atoms incorporated into the CNT walls. The feature III corresponds to the trapped N_2 molecules.[24] Fitting of N 1s spectrum with Gaussian functions showed that the incorporation of nitrogen atoms in CNTs occurred predominantly by direct substitution of carbon atoms (~54.4%). The relative proportions of pyridinic and molecular forms are about 21.0% and 24.5%, respectively.

B. Polystyrene composite preparation

Polystyrene composites with CNTs, both pure and nitrogen-doped, were prepared by a forge rolling method developed previously by Gavrilov *et al.*[25,26] for composites filled with onion-like carbon, and by Kanygin *et al.*[27] and Okotrub *et al.*[28] for CNT-based composites. It was shown that shear deformation applied during the composite preparation disentangles the nanoparticles from their agglomerates (see Ref. 25) and distributes the filler evenly.[26] Moreover, as it was shown by Kanygin *et al.*[27] that repeated forge rolling in a given direction results in a predominant orientation of the nanotubes in polymer matrix, providing anisotropy of both the structure and the macroscopic properties of the composite.

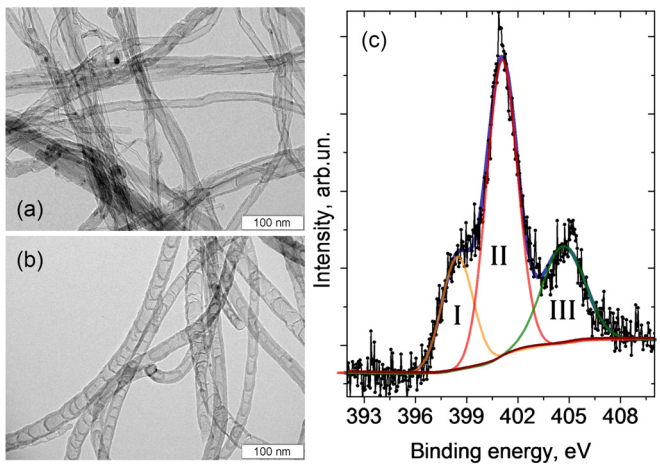

FIG. 1. TEM images of MWCNTs (a) and N-MWCNTs (b). XPS N 1 s spectrum of N-MWCNT sample fitted by three Gaussian-like components (c).

Arrays of nanotubes were gently detached from silicon substrates and stirred carefully with polystyrene in toluene solution until complete dissolution of the polymer. The obtained composite materials were coated on a metallic plate and dried at room temperature during 3 h for viscosity increase, and the samples were repeatedly forge-rolled along one direction. Then, the sample plates were dried under light load at room temperature. The thickness of plate (20 mm × 30 mm in square) varied from 300 to 700 μm. MWCNT/polystyrene and N-MWCNT/polystyrene composites with 0.5, 1.0, 2.0, 3.0, and 4.0 wt. % loading were prepared.

Assuming that the forge rolling results in predominant alignment of MWCNTs along a composite plate, we reoriented the nanotubes using the following procedure. Composite plate was cut across the rolling direction into strips ~15 mm in length and ~1.5 mm in width, and thickness of 300–700 μm. The strips were rotated through 90° and then glued together face to face by toluene. An assembly plate was dried at room temperature during 4–6 h and then polished mechanically. It was expected that, as a result of the preparation procedure, the nanotubes would be normally oriented to sample surface while the composite loading will be unchanged as compared to the origin polymer plate.

Okotrub *et al.*[28] suggested that strong forces of the rolls could break the nanotubes. To check the veracity of this effect, the polystyrene matrix of a few polymer plates was dissolved in toluene and nanotubes were extracted. Sediments so obtained were investigated by TEM (Figs. 2(a) and 2(b)). Statistical analysis of the images confirms the shortening of the length of both types of nanotubes down to about 0.5–2.5 μm in the composites prepared by the forge rolling procedure (Fig. 2(c)). The similar length distribution could indicate that pure MWCNTs and nitrogen-doped MWCNTs are close in mechanical strength, and even if there was difference, it is negligible as compared with the forces acting on the nanotubes at the forge-rolling.

C. Phosphate composite preparation

Unfired phosphate ceramics, consisting of aluminum-phosphate binder and filler containing corundum (α-Al_2O_3) and aluminum nitride, developed by Corpus *et al.*[29] and Krylova *et al.*[30] has been used as a host for CNT/phosphate composites fabrication. These composites present outstanding thermal stability and mechanical strength.

Aluminum-phosphate binder was prepared by dissolving aluminum hydroxide in a solution of phosphoric acid with a mass fraction of 60%. The molar ratio $H_3PO_4/Al(OH)_3$ was taken equal to 3. Dissolution was carried out with continuous stirring and gentle heating (80–90 °C) until obtaining a clear homogeneous solution. After cooling to room temperature, the solution was diluted with water to a density equal to 1.35–1.45 g/cm^3. The filler was a homogeneous mixture of

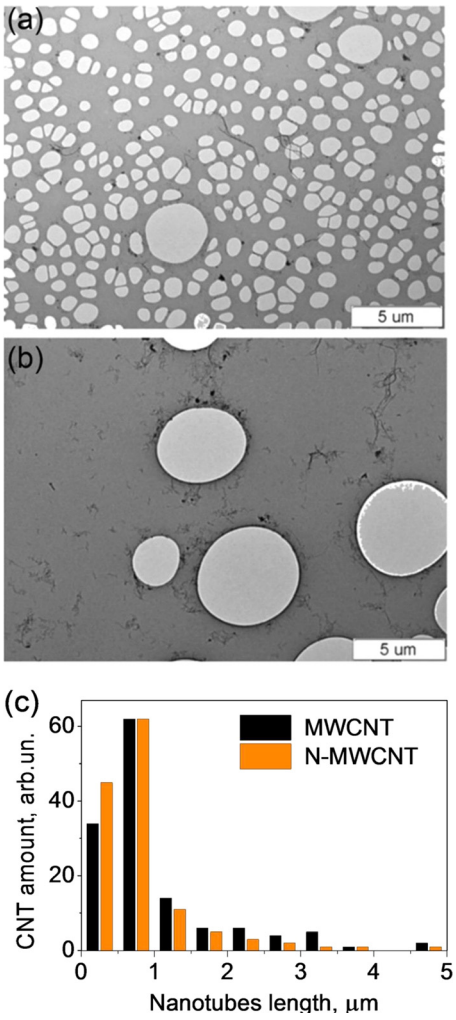

FIG. 2. TEM images of sediments of MWCNTs (a) and N-MWCNTs (b) extracted from composite by polystyrene dissolving. Length distribution of MWCNTs and N-MWCNTs after rolling procedure (c).

powders of aluminum oxide and aluminum nitride with a mass ratio of 9:1.

MWCNTs or N-MWCNTs used as functional additive, filler and aluminum-phosphate binder have been grinded during 3–4 min in agate vessel. Once homogenized, the samples were pressed as 2 mm thick tablets of 10 mm in diameter. The compacting pressure was 50 kg/cm^2. Heat treatment was performed at 80 °C. MWCNT/phosphate and N-MWCNT/phosphate composites with 0.25, 0.5, 1.0, and 1.5 wt. % loading were prepared. SEM observations (see Fig. 3) suggest that the used procedure could result in homogeneous distribution of isolated nanotubes, which are shorter that the initial ones due to the grinding. Attempts to fill in phosphate host with more than 1.5 wt. % CNTs were not successful because the nanotubes distribution in that case was not adequately uniform.

D. Measurement technique

Impedance real and imaginary parts of MWCNT/polystyrene and N-MWCNT/polystyrene composites in static regime were measured by two-contact method with an impedance meter Z–2000 (made by "Elins," Chernogolovka, Russia). The sample was placed in the central part of the measurement cell. Reconstruction of the dielectric permittivity from the measured impedance was done as described by Gavrilov *et al.*[26] The dielectric response of polymer composites was measured twice: before and after reorientation of nanotubes in the samples. In the former case, nanotubes lay along the composite plate surface, which was perpendicular to the electric field (MWCNT⊥E, N-MWCNT⊥E). Otherwise, in the reoriented composites the nanotubes stacked normally to the plate surface, and hence they were parallel to the electric field (MWCNT||E, N-MWCNT||E).

The *dc* resistance of phosphate composites was measured using two-point method in a two-probe pressure cell using measuring bridge R3009 (up to $1.1 \times 10^{10}\,\Omega$). Electrical contacts were realized by using graphite glue.

The microwave measurements for phosphate composites were provided by scalar network analyzer R2–408R (ELMIKA, Vilnius, Lithuania), including sweep generator, waveguide reflectometer, and indicator unit (personal computer). The IEC 62431:2008(E) standard specifying the measurement method for the reflectivity of EM materials

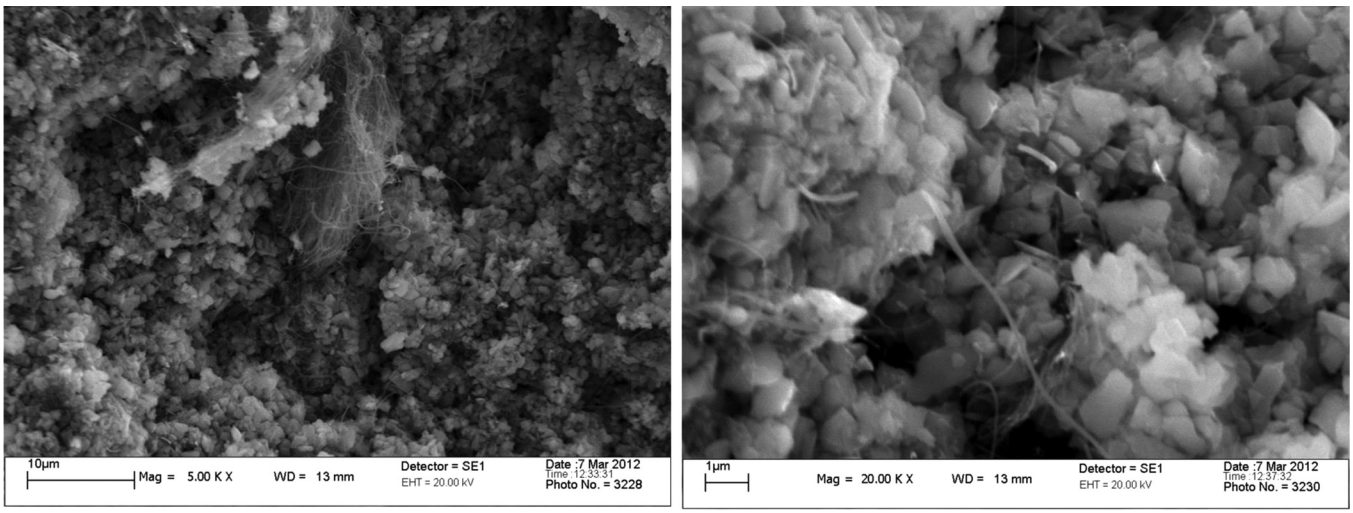

FIG. 3. SEM images of MWCNT/phosphate composites with 1.5 wt. % loading.

was used. The EM responses of the samples defined as the ratios of transmitted/input (S_{21}) and reflected/input (S_{11}) signals have been measured within 26–37.5 GHz frequency range (K_a–band). The frequency stability of the oscillator was controlled by frequency meter and was achieved at the level of 10^{-6}. The power stabilization was maintained at 7.0 MW ± 10 μW. The measurement range of the EM attenuation was from 0 to −40 dB. Measurement error of the EM attenuation was 7%. The accuracy has been controlled by repetitive measurements for different orientations of the sample in the waveguide cross-section. The samples were cut precisely to fit the waveguide cross-section 7.2 × 3.4 mm. The measurements were performed with free-standing samples.

III. MEASUREMENT RESULTS

A. Static regime

The experimental values of the dielectric permittivity ε of polystyrene composites *vs* CNT concentration are shown in Fig. 4. The enhancement of composite permittivity with the sample reorientation indicates an alignment of the nanotubes in polymer matrix with the rolling direction. For the same content of MWCNTs, the permittivity of the reoriented composites (MWCNT||E) is two or three times larger than that of the just-rolled samples (MWCNT⊥E) and is about four times as large as that of pure polystyrene matrix ($\varepsilon^{\text{polystyrene}} = 1.9$). This effect is considerably less pronounced for the N-MWCNTs as far as one can judge from the invariability of the perpendicular dielectric response with increasing nanotube content up to 4 wt. %. Reorientation results in almost doubling the ε value.

Table I presents *dc* conductivity reconstructed from the experimental data for MWCNT/phosphate composites. *dc* conductivity measured for phosphate composites filled with N-MWCNT for all concentrations (0.25–1.5 wt. %) was found to be the same as for the unloaded phosphate matrix (at the level of 10^{-12} S/cm).

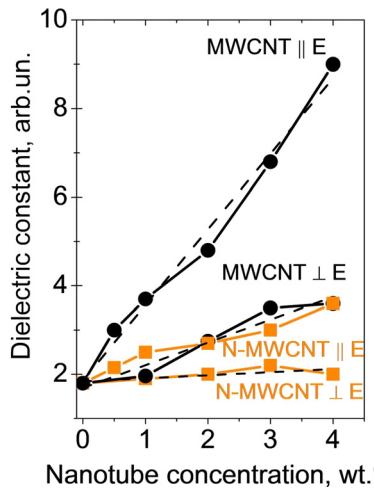

FIG. 4. Static dielectric permittivity of MWCNT/polystyrene and N-MWCNT/polystyrene composites measured for electric field polarized parallel (CNT||E) and perpendicular (CNT⊥E) to the rolling direction.

TABLE I. *dc* conductivity in logarithmic scale for CNT/phosphate composites.

MWCNT concentration	0	0.25	0.5	1.0	1.5
$\text{Log}_{10}(\sigma)$	−12.00	−8.95	−8.58	−3.91	1.02

B. Microwave probing

Electromagnetic interference shielding effectiveness (EMI SE), $-S_{21}$, and $-S_{11}$ parameters (corresponding to the CNT-based phosphates reflectance capability) *vs* N-MWCNT content measured in K_a–band is presented in Fig. 5(a). Reflection (R), transmission (T), and absorption (A) are related to the measured S–parameters in the following way: $R = S_{11}^2$, $T = S_{21}^2$, and $A = 1 - R - T$. Both measured T and R and calculated A values are presented in Fig. 5(b) for N-MWCNT/phosphate composites and the T value provided by pure MWCNTs added to phosphate host with the same concentration is also presented in the same figure for comparison. The EM attenuation of microwave radiation (S_{21}) of the N-MWCNT/phosphate composites is small for 2 mm thick layer, not higher than 5 dB, and determined mostly by the EM response of the pure phosphate matrix. The whole observed SE (defined as the reciprocal transmission factor) is the combination of the absorption of the EM energy, the reflection from the material surface and multiple internal reflections of the EM radiations. For the N-MWCNT/phosphate composites, the reflectance and transmittance have nearly constant values ($R^{\text{N-MWCNT/phosphate}} \approx 44\%$, $T^{\text{N-MWCNT/phosphate}} \approx 55\%$) and the absorption is less than 7%. In contrast, MWCNTs added to phosphate matrix with the same concentration provide extremely high EM attenuation in microwave range, increasing monotonously with the CNT concentration: 1.0 wt. % of pure MWCNT in phosphate allows only 20% of microwave radiations to pass through the 2 mm thick sample; 1.5 wt. % MWCNT makes phosphate matrix almost opaque for EM radiation in the K_a–band.

IV. POLARIZABILITY MODELING

Dielectric properties of composite are governed by (1) the content and distribution of the filler in the matrix and (2) the geometry and electronic structures of the embedded nanoparticles. The similarity in the preparation procedures of CNT- and N-CNT-based composites eliminates the influence of the first factor. At the same time, the microstructure of the nanotubes depends on an ensemble of parameters. Addition of nitrogen-containing compound into feedstock leads to an alteration of the CVD processes and formation of highly defective nanotubes incorporating nitrogen in different bonding configurations. In the present section, we analyze effects of nanotube defect-free-length and nitrogen impurities on the polarizability.

A. Length dependence

As shown by Benedict *et al.*,[31] Brothers *et al.*,[32,33] and Kozinsky and Marzari,[34] the dielectric properties of a

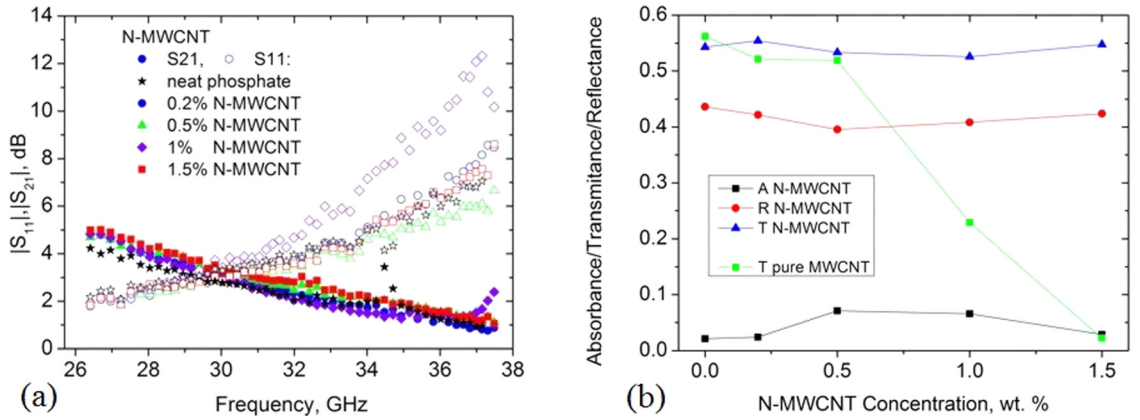

FIG. 5. S_{21} and S_{11} of N-MWCNT/phosphate composites in frequency range 26–37 GHz (a). Transmittance, absorbance, and reflectance of MWCNT/phosphate and N-MWCNT/phosphate composites in microwave ranges (30 GHz) (b).

nanotube crystal is governed by the axial component of the tube polarizability $\alpha_{\|}$ and, to a lesser extent, to the transverse one $\alpha_{\perp}$, which in turn depends on the geometry (radius R and length L) and the electronic structure (band gap E_g) of the nanotubes as

$$\alpha_{\perp}/L \sim R^2, \quad \alpha_{\|}/L \sim R/{E_g}^2. \tag{1}$$

Using Eqs. (1) and known geometrical parameters of nanotubes (see Sec. II B) in rolled polymer composites, one can see that, as a result of nitrogen doping, the values of both the axial and transverse components of the nanotube polarizability should at least double. Change in the polarization response of the nanotubes due to the doping can be estimated from the experimental dielectric data as

$$\alpha^{\mathrm{MWCNT}}{}_{\perp,\|}/\alpha^{\mathrm{N-MWCNT}}{}_{\perp,\|} = \left(\varepsilon^{\mathrm{composite}}{}_{\perp,\|} - \varepsilon^{\mathrm{matrix}}\right)^{\mathrm{MWCNT}}/\left(\varepsilon^{\mathrm{composite}}{}_{\perp,\|} - \varepsilon^{\mathrm{matrix}}\right)^{\mathrm{N-MWCNT}}. \tag{2}$$

For polystyrene composites containing 4 wt. % nanotubes, Eq. (2) indicates that the axial and perpendicular polarizabilities of N-MWCNTs are approximately eight and four times smaller than the corresponding values of MWCNTs.

The axial polarizability of MWCNTs, $\alpha(\omega)$ shown in Fig. 6 for a particular nanotube geometry, was calculated rigorously using the idea of CNT as transmission line developed by Slepyan *et al.*[35] within the linear nanoelectrodynamics for zigzag, armchair, and chiral CNT in the

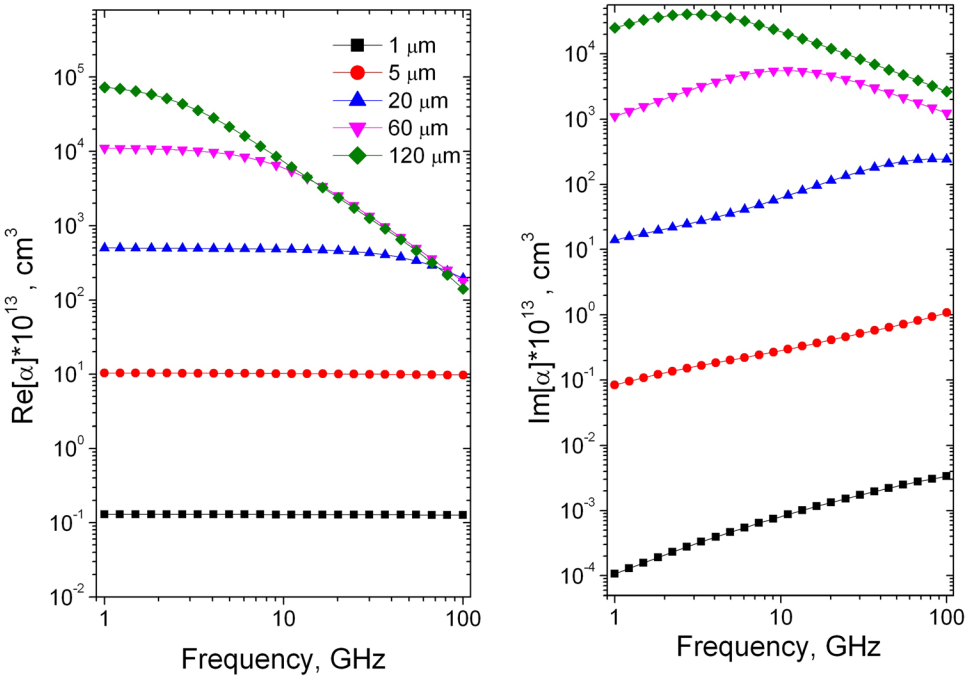

FIG. 6. Frequency dependence of the real and imaginary parts of the axial polarizability of MWCNT on length.

microwave and THz frequency regimes and by applying the integral equations technique described by Shuba *et al.*[36] According to realistic geometry of MWCNTs more appropriate to our experiments, calculations were done for long CNTs (20–120 μm) of 20 nm diameter and for short CNTs (5 and 1 μm) of 50 nm diameter. The electron relaxation time required by the theory was set at 4×10^{-14} s for the MWCNTs. One can see (Fig. 6) that the polarizability of long CNTs (60–120 μm) is higher in microwave frequency range (30 GHz) than the polarizability of short ones (1 μm) by more than 4 orders of magnitude.

B. Effect of nitrogen defects

The influence of CNT functionalization (nitrogen doping in our case) could be important only when comparing nanotubes of the same length as we have in forge-rolled composites. According to the XPS data (see Sec. II A), the composition of N-MWCNTs used for composites preparation is $CN_{0.04}$. The N_2 molecules, trapped between nanotube layers or located in nanotube cavities, should give negligible effect on the polarizability due to screening effect by the outermost shells. Ignoring therefore the molecular form of nitrogen, we have constructed a nanotube model with composition $CN_{0.03}$. The model is based on an armchair (6,6) CNT with five hexagon rings in length and both ends closed by hemispherical caps (Fig. 7(a)). To keep the 2:1 ratio between graphitic and pyridinic nitrogen forms, four carbon atoms were directly replaced by nitrogen atoms and two nitrogen atoms were located at the boundary of a lattice vacancy. Graphitic nitrogen impurities were inserted in the pentagonal rings, forming two para-defects located at the opposite tube caps, because, as it has been shown by Bulusheva *et al.*,[37] these sites are energetically preferable. To separate the contributions of the different forms of nitrogen, we considered also the $CN_{0.01}$ model sketched in Fig. 7(b), which contains only piridinic-like defects. Moreover, the pure carbon model (armchair (6,6) CNT with one mono-vacancy)

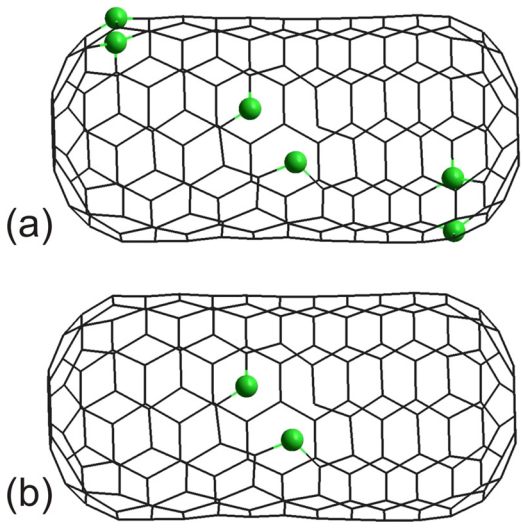

FIG. 7. Models of nitrogen-containing armchair (6,6) CNT: $CN_{0.03}$ tube with four graphitic and two pyridinic nitrogen atoms (a), $CN_{0.01}$ tube with two pyridinic nitrogen atoms (b). The nitrogen atoms are highlighted.

TABLE II. Static polarizability α of the nanotube models calculated at the CPKS/B3LYP/6-31G(*+) level.

Model	CNT	$CN_{0.01}$	$CN_{0.03}$
α, Å^3	330.1	328.8	337.1

was calculated for the comparison. The calculations were performed using the three-parameter hybrid functional of Becke[38] and the Lee-Yang-Parr correlation functional[39] (B3LYP method) included in the JAGUAR program package.[40] The atomic positions in the models were relaxed using an analytic procedure until the gradient values get smaller than $5 \cdot 10^{-5}$ Hartree/bohr. Atomic orbitals were described by the 6–31G basis set. The static polarizability of nanotube models was defined as one third of the trace of the polarizability tensor calculated by solving the coupled-perturbed Kohn-Sham (CPKS) equations at the B3LYP/6-31G^{*+} level (polarization and diffuse wavefunctions included).

Our calculations show that the static polarizability α of N-CNT depends on the form of the incorporated nitrogen (Table II). Pyridinic nitrogen is unfavorable for the CNT polarization: the α value decreases by $\sim$1.3 Å^3 relative to the pure-carbon model with single-vacancies. Direct nitrogen atoms substitution for carbon atoms (graphitic nitrogen), on the other hand, enhances the static polarizability. The α value obtained for the $CN_{0.03}$ model is by $\sim$7 Å^3 larger than that for the pure carbon counterpart.

V. DISCUSSION

Experimental investigations of the electrical conductivity of N-doped CNTs yield ambiguous conclusions on the influence of nitrogen doping on the electromagnetic properties of CNTs. Ismagilov *et al.*[16] and Villalpando-Paez *et al.*[15] observed improvement of conductivity of CNTs and nanofibers with nitrogen doping. Other authors (Krstić *et al.*[41] and Ibrahim *et al.*[42]) found deterioration of the electrical transport properties of N-CNTs over the pure carbon ones. Our measurements show that adding N-MWCNTs does not increase the permittivity and the EM attenuation ability of a composite in all the investigated concentration range. From theoretical considerations, two main structural features of N-MWCNTs could be responsible for this result.

First, the as-prepared N-MWCNTs always contain incorporated nitrogen atoms in different forms. Our *ab-initio* calculations reveal that the static polarizability of CNT can both increase and decrease with nitrogen doping depending on the N incorporation form (Table II). The calculations predict an enhancement of the polarizability for graphitic nitrogen, which is in agreement with the published literature. Particularly, theoretical investigations of Nemilentsau *et al.*[17] related that nitrogen substitutional doping narrows the current gap in semiconducting CNTs and leads to electron backscattering in the initially metallic CNTs. In the case of an armchair SWCNT, Green's function DFT calculations demonstrated (see Ref. 43) that a nitrogen substitutional defect does not affect the intrinsic conductivity of the nanotube. The substitutional doping of an initially

semiconducting zigzag nanotubes was predicted by Latil *et al.*[19] to enhance its axial polarizability. Alternatively, our calculations predict a decrease in the static polarizability of a CNT with the pyridinic nitrogen formation (Table II). And this result is in accordance with an appearance of energy band gap for an armchair CNT contained pyridinic nitrogen defects (see Ref. 44).

Second, the N-MWCNTs often have bamboo-like structure. Comparing the theoretical results (Fig. 6) and experimental data (Fig. 5), we conclude that the determinant contribution to the microwave response is the tube effective length. The high-frequency polarizability α is exceptionally higher for the long CNTs. Bamboo-like N-MWCNTs, studied here consist of a more-or-less periodical stack of cones with length of 50–70 nm (Fig. 1(b)) that could create additional structural defects in the nanotube walls. For that reason, it is likely that the N-MWCNTs have shorter defect-free-length than the non-doped MWCNTs and this geometrical effect could hinder any enhancement of the high-frequency polarizability due to the nitrogen substitutional doping. The results for N-MWCNT-based composites collected in microwave range are supported by *dc* conductivity data (see Sec. III A), where in contrast to theoretical estimations for N-CNT polarizability being in some cases higher than for pure ones (see Ref. 19), we observe a dramatic suppression of conductance ability of N-MWCNTs in comparison with the non-doped ones.

To exploit all the potential of nitrogen doping in enhancing the electromagnetic response of CNTs, the aforementioned structural effects should be corrected. Because the graphitic nitrogen is more thermodynamically stable than the pyridinic one (see Ref. 45), sufficient enrichment in the first form could be achieved with high-temperature annealing of the sample. This processing would also decrease the number of other structural defects, such as topological defects and sp^3-hybridized carbon atoms, thus increasing the defect-free areas in the external CNT walls. Bamboo-like structure is usually observed for N-MWCNTs; hence, the double-walled or few-walled CNTs having straight, non-buckled walls (see Ref. 46) similar to their non-doped counterparts are recommended for the post-synthesis treatment.

VI. CONCLUSION

We have performed dielectric and microwave (26–37.5 GHz) analysis of composites filled with MWCNTs and N-MWCNTs. Two classes of host matrix—polystyrene and phosphate unfired ceramics—have been used as host matrices. We found an increase in the dielectric permittivity of polystyrene with MWCNT addition, especially when nanotubes have a predominant orientation in the matrix. Phosphate ceramics containing 1.5 wt. % pristine MWCNTs demonstrated relatively high EMI SE at the level of 95% attenuation of incident microwave power. In contrast to pure MWCNTs, the nitrogen-doped ones were observed to have a little effect on the electromagnetic properties of both types of composites. Quantum chemistry calculations can explain this observation as being the results of (1) a decrease of the defect-free-length due to the bamboo-like structure of N-MWCNTs and (2) the incorporation of nitrogen atoms into the CNT walls in pyridinic form. Thus, by changing the MWCNT fillers by N-MWCNTs, one could create composites with gradient or modulating electromagnetic response.

In spite of the fact that nitrogen doped CNTs does not have significant impact to EM shielding effectiveness of composites in microwave frequency range, they posses promising properties in optical frequencies: it was shown in the recent comprehensive review of Jana *et al.*,[47] both theoretically and experimentally, that N-CNTs demonstrate novel electronic and optical properties that are not observed in pure CNTs, and therefore in near future Jana *et al.*[47] expected N-CNTs to be more useful, interesting and challenging than the un-doped ones. At the same time, Jana *et al.*[47] stress that it is necessary to repeat the experiments to understand clearly the mechanisms and processes related to different physical properties of the doped systems. One of the steps to follow this advice has been done in the present paper.

ACKNOWLEDGMENTS

This research was partly funded by the EU FP7 projects PIRSES-GA-2012-318617 FAEMCAR and FP7-266529 BY-NanoERA, as well as the BRFFI project (F12R–030) and the RFBR project (grant 12-02-90011). The work of M. A. Kanygin was also partly supported by the "UMNIK" program of FASIE-Foundation.

[1]F. Qin and C. Brosseau, J. Appl. Phys. **111**, 061301 (2012).
[2]D. D. L. Chung, Carbon **50**(9), 3342 (2012).
[3]W. Bauhofer and J. Kovac, Compos. Sci. Technol. **69**(10), 1486 (2009).
[4]P. Kuzhir, A. Paddubskaya, D. Bychanok, A. Nemilentsau, M. Shuba, A. Plusch, S. Maksimenko, S. Bellucci, L. Coderoni, F. Micciulla, I. Sacco, G. Rinaldi, J. Macutkevic, D. Seliuta, G. Valušis, and J. Banys, Thin Solid Films **519**(2), 4114 (2011).
[5]C. Zhou, J. Kong, E. Yenilmez, and H. Dai, Science **290**, 1552 (2000).
[6]H. Khalfoun, P. Hermet, L. Henrard, and S. Latil, Phys. Rev. B **81**, 193411 (2010).
[7]P.-C. Ma, N. A. Siddiqui, G. Marom, and J.-K. Kim, Composites, A **41** (10) 1345 (2010).
[8]J. Li, P.-C. Ma, W. S. Chow, C. K. To, B. Z. Tang, and J.-K. Kim, Adv. Funct. Mater. **17**(16) 3207 (2007).
[9]A. Mayer, Phys. Rev. B **75**(4), 045407 (2007).
[10]M. Zdrojek, T. Heim, D. Brunel, A. Mayer, and T. Melin, Phys. Rev. B **77**(3), 033404 (2008).
[11]M. V. Shuba, G. Ya. Slepyan, S. A. Maksimenko, and G. W. Hanson, J. Appl. Phys. **108**, 114302 (2010).
[12]P. P. Kuzhir, A. G. Paddubskaya, M. V. Shuba, S. A. Maksimenko, A. Celzard, V. Fierro, G. Amaral-Labat, A. Pizzi, G. Valušis, J. Macutkevic, M. Ivanov, J. Banys, S. Bistarelli, A. Cataldo, M. Mastrucci, F. Micciulla, I. Sacco, E. Stefanutti, and S. Bellucci, J. Nanophotonics **6**, 061715 (2012).
[13]R. Czerw, M. Terrones, J.-C. Charlier, X. Blase, B. Foley, R. Kamalakaran, N. Grobert, H. Terrones, D. Tekleab, P. M. Ajayan, W. Blau, M. Rühle, and D. L. Carroll, Nano Lett. **1**(9), 457 (2001).
[14]C. P. Ewels and M. Glerup, J. Nanosci. Nanotechnol. **5**, 1345 (2005).
[15]F. Villalpando-Paez, A. Zamudio, A. L. Elias, H. Son, E. B. Barros, S. G. Chou, Y. A. Kim, H. Muramatsu, T. Hayashi, J. Kong, H. Terrones, G. Dresselhaus, M. Endo, M. Terrones, and M. S. Dresselhaus, Chem. Phys. Lett. **424**(4–6), 345 (2006).
[16]Z. R. Ismagilov, A. E. Shalagina, O. Yu. Podyacheva, A. V. Ischenko, L. S. Kibis, A. I. Boronin, Yu. A. Chesalov, D. I. Kochubey, A. I. Romanenko, O. B. Anikeeva, T. I. Buryakov, and E. N. Tkachev, Carbon **47**, 1922 (2009).

[17]A. M. Nemilentsau, M. V. Shuba, G. Ya. Slepyan, P. P. Kuzhir, S. A. Maksimenko. P. N. D'yachkov, and A. Lakhtakia, Phys. Rev. B **82**, 235424 (2010).
[18]E. Xu, J. Wei, K. Wang, Z. Li, X. Gui, Yi. Jia, H. Zhu, and D. Wu, Carbon **48**(11), 3097 (2010).
[19]S. Latil, S. Roche, D. Mayou, and J.-C. Charlier, Phys. Rev. Lett **92**, 256805 (2004).
[20]A. V. Okotrub, L. G. Bulusheva, A. G. Kudashov, V. V. Belavin, and S. V. Komogortsev, Nanotechnol. Russ. **3**, 191 (2008).
[21]G. Y. Zhang, X. C. Ma, D. Y. Zhong, and E. G. Wang, J. Appl. Phys. **91**, 9324 (2002).
[22]A. V. Okotrub, L. G. Bulusheva, A. G. Kudashov, V. V. Belavin, D. V. Vyalikh, and S. L. Molodtsov, Appl. Phys. A **94**(3), 437 (2009).
[23]A. G. Kudashov, A. V. Okotrub, L. G. Bulusheva, I. P. Asanov, Y. V. Shubin, N. F. Yudanov, V. S. Danilovich, and O. G. Abrosimov, J. Phys. Chem. B **108**, 9048 (2004).
[24]H. C. Choi, J. Park, and B. Kim, J. Phys. Chem. B **109**, 4333 (2005).
[25]N. N. Gavrilov, A. V. Okotrub, L. G. Bulusheva, V. L. Kuznetsov, and S. I. Moseenkov, Tech. Phys. Lett. **35**, 85 (2009).
[26]N. N. Gavrilov, A. V. Okotrub, L. G. Bulusheva, O. V. Sedelnikova, I. V. Yushina, and V. L. Kuznetsov, Compos. Sci. Technol. **70**, 719 (2010).
[27]M. A. Kanygin, A. G. Selyutin, A. V. Okotrub, and L. G. Bulusheva, Fullerenes, Nanotubes, Carbon Nanostruct. **20**, 523 (2012).
[28]A. V. Okotrub, V. V. Kubarev, M. A. Kanygin, O. V. Sedelnikova, and L. G. Bulusheva, Phys. Status Solidi B **248**, 2568 (2011).
[29]V. A. Corpus, Z. F. Krylova, L. I. Dorozhkina, V. F. Tikavy, I. A. Zakharov, and G. A. Shevergina, "Refractory mixture," patent 2,035,432 (2 May 1995), RU, Bulletin No. 14.
[30]Z. Ph. Krylova, L. I. Dorozhkina, I. A. Zakharov, A. E. Bazarov, V. A. Corpus, and V. F. Tikavy, "High-temperature glue composition," patent 2,066,335 (10 September 1996), RU, Bulletin No. 25.
[31]L. X. Benedict, S. G. Louie, and M. L. Cohen, Phys. Rev. B **52**, 8541 (1995).
[32]E. N. Brothers, K. N. Kudin, G. E. Scuseria, and C. W. Bauschlicher, Jr., Phys. Rev. B **72**, 033402 (2005).
[33]E. N. Brothers, G. E. Scuseria, and K. N. Kudin, J. Phys. Chem. B **110**, 12860 (2006).
[34]B. Kozinsky and N. Marzari, Phys. Rev. Lett. **96**, 166801 (2006).
[35]G. Ya. Slepyan, S. A. Maksimenko, A. Lakhtakia, O. M. Yevtushenko, and A. V. Gusakov, Phys. Rev. B **60**, 17136 (1999).
[36]M. V. Shuba, G. Ya. Slepyan, S. A. Maksimenko, C. Thomsen, and A. Lakhtakia, Phys. Rev. B **79**(15), 155403 (2009).
[37]L. G. Bulusheva, O. V. Sedelnikova, and A. V. Okotrub, Int. J. Quantum Chem. **111**, 2696 (2011).
[38]A. D. Becke, J. Chem. Phys. **98**, 5648 (1993).
[39]C. Lee, W. Yang, and R. G. Parr, Phys. Rev. B **37**, 785 (1988).
[40]JAGUAR, version 7.8, Schrödinger, LLC, New York, NY, 2011.
[41]V. Krstić, G. L. J. A. Rikken, P. Bernier, S. Roth, and M. Glerup, Europhys. Lett. **77**, 37001 (2007).
[42]E. M. M. Ibrahim, V. O. Khavrus, A. Leonhardt, S. Hampel, S. Oswald, M. H. Rümmeli, and B. Büchner, Diamond Relat. Mater. **19**, 1199 (2010).
[43]H. J. Choi, J. Ihm, S. G. Louie, and M. L. Cohen, Phys. Rev. Lett. **84**, 2917 (2000).
[44]J.-X. Zhao, Y.-H. Ding, X.-G. Wang, Q.-H. Cai, and X.-Z. Wang, Diamond Relat. Mater. **20**, 36 (2011).
[45]L. G. Bulusheva, A. V. Okotrub, I. A. Kinloch, I. P. Asanov, A. G. Kurenya, A. G. Kudashov, X. Chen, and H. Song, Phys. Status Solidi B **245**, 1971 (2008).
[46]P. Ayala, A. Gru1neis, T. Gemming, D. Grimm, C. Kramberger, M. H. Rümmeli, F. L. Freire, Jr., H. Kuzmany, R. Pfeiffer, A. Barreiro, B. Büchner, and T. Pichler, J. Phys. Chem. C **111**, 2879 (2007).
[47]D. Jana, C.-L. Sun, L.-C. Chen, and K.-H. Chen, Prog. Mater. Sci. **58**, 565 (2013).